Bridging the gap between the Darcy-Brinkman equations and the Nielsen model for tortuosity in polymer-filled systems

C. Varsakelis, M.V. Papalexandris

Institute of Mechanics, Materials and Civil Engineering
UCLouvain
Place du Levant 2, B-1348 Louvain-la-Neuve
Belgium

Abstract

The present study establishes the link between the well-known Nielsen model for the calculation of tortuosity in polymer-filled systems and the Darcy–Brinkman equation for flows in porous media. Based on the fact that the polymer-filled system is a porous medium, with properties fixed by the volume fraction and the geometry of the fillers, we employ the Darcy-Brinkman equations to compute an expression for tortuosity. This expression is then directly linked to the interphasial drag coefficient. Finally, we prove that the Nielsen model constitutes a special case of our derived formula.

Keywords: Polymer filled systems, Tortuosity, Darcy-Brinkman equation, porous media

1. Introduction

It is well known that the addition of inorganic impermeable particles (fillers) in a polymer matrix can substantially modify both the gas and water-vapor permeability properties of the resulting polymer-filled system, [1, 2]. The exact mechanism is quite complex and a complete understanding requires the study of adhesion, diffusion, solubility and others, [3]. However, for uncharged particles,

Email address: christos.varsakelis@uclouvain.be, miltos@uclouvain.be (M.V. Papalexandris)

the improvement of barrier properties is dominated by a decrease in diffusivity due to changes in tortuosity, a purely geometric quantity defined as the average diffusion length of molecules in the system. Indeed, more than fifty years ago, the authors of [4] showed that the addition of impermeable particles transforms the path of diffusive molecules from a straight line to a tortuous one which, as expected, depends on the volume fraction of the particles, their shape and their configuration in space, [5]. In other words, the addition of fillers in the polymer matrix results in an increase of tortuosity.

Theoretical efforts to calculate tortuosity in polymer-filled systems have a long history. In a seminal article, [6], Nielsen considered the case of planar, monodisperse and homogeneously distributed particles. By using a simple averaging argument he demonstrated that tortuosity is a linear function of the volume fraction and the aspect ratio of the particles. This strikingly simple correlation is formally valid for low volume fractions and high-aspect ratio particles (needle-like shapes). Comparisons against experimental measurements and detailed numerical simulations have proven that, within its domain of validity, the Nielsen model has a good predictive capacity [7, 3, 8]. Of course, in applications, one is often confronted with scenarios that go beyond the simple framework that Nielsen considered. Although efforts to utilize the Nielsen model in more general settings have been made, in such situations, the traditionally physical constants, necessarily, become fitting parameters. In turn, this prompted the extension of the initial model to more general cases, allowing for formally accounting for higher volume fractions, polydispersity, orientation flexibility, variations in shapes etc. The relevant literature is quite long and we, therefore, refer to the recent works of [9, 10] for systematic and critical reviews that also offer a wealth of additional references.

Despite the presence of more elaborate avatars, the Nielsen model constitutes a simple, albeit elegant, first-order approximation of tortuosity. With this in mind, the present study establishes the formal link between the Nielsen model and the Darcy–Brinkman equation for flows in porous media.

Our starting point is the observation that the polymer-filled system consti-

tutes a porous medium whose porous skeleton is defined by the characteristics and volume fraction of the fillers. We then utilize the Darcy-Brinkman equations for the calculation of the velocity profile inside the porous medium. What renders our analysis challenging is the fact that, by employing the Darcy-Brinkman equations, we inherit both a macroscopic scale, related to the domain of the porous medium, and a microscopic scale, related to the characteristic scales of the porous skeleton. In order to circumvent this obstacle, we subtly average the velocity profile over a range that is i) small enough to isolate boundary effects and ii) large enough to maintain the validity of Darcy–Brinkman equations. This range is determined by the boundary layer analysis of the Darcy-Brinkman equations previously performed in [11, 12]. Expressions for tortuosity are then obtained as the ratio of this, averaged, velocity over the, again averaged, velocity profile in the absence of a porous medium (pure fluid).

With the theoretical expressions for the tortuosity at hand, we proceed further and juxtapose them with those of the Nielsen model. Our analysis asserts that the Nielsen model can be recovered from Darcy–Brinkman equation as a special case.

Our approach constitutes the macroscopic and homogenized analogue of the one employed in [13, 14, 15]; see also the recent review article [16]. In those articles, the authors used Lattice-Boltzmann (LB) simulations at sub-pore scales and reconstructed tortuosity through averaging of the corresponding streamlines. The advantage of LB simulations is that they can deal with very complicated porous skeletons, for which expressions for the interphasial drag may not be available. However, for the case of interest, our approach offers a viable alternative especially since all the necessary quantities can be analytically computed.

The paper is organized as follows. In section 2 we present a critical evaluation of the Nielsen model. Section 3 deals with the derivation of tortuosity estimates, based on the Darcy-Brinkman equations, whereas section 4 includes a comparison and analysis of the theoretical expressions and their implications. Finally, section 5 concludes.

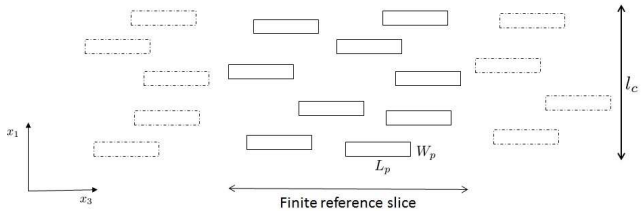


Figure 1: The polymer-filled system configuration that the Nielsen model deals with. Solid-line fillers live in the domain where the analysis takes please whiled dashed ones live outside and illustrate the infinite extension in the normal direction.

2. The Nielsen model

The Nielsen model, originally derived by Nielsen in [6], concerns the diffusion of a gaseous phase through a planar polymer matrix that is of finite length $\hat{l}_c$ in the diffusion (streamwise) direction and extends indefinitely in the normal direction (infinite width $\hat{w}_c$) or equivalently being periodic; here and in what follows, a hat symbol "ˆ" above a variable will denote that the variable is dimensional and likewise variables without a hat symbol are non-dimensional. In this polymer matrix a collection of monodisperse fillers, with width $\hat{W}_p$ and length $\hat{L}_p$, is homogeneously added so that the length is perpendicular to the streamwise direction and the total particle volume fraction is $\phi_p > 0$. This configuration is depicted in Figure 1.

Nielsen's model is based on the following rationale. While diffusing through polymer-filled system, a gas molecule will encounter, on average, $\hat{l}_c \phi_p \hat{W}_c$ particles and each particle adds, again on average, $\hat{L}/2$ of extra distance. Consequently, the total distance traveled by the average gas molecule is,

$$\hat{l}_p = \hat{l}_c \left(1 + \frac{1}{2} \phi_p \frac{\hat{L}_p}{\hat{W}_p} \right) .$$

Let $a_p = \hat{L}_p / \hat{W}_p$ designate the aspect ratio of the particles. Then, it readily follows that the tortuosity τ_N is given by

$$\tau_N = 1 + \frac{1}{2} \phi_p a_p \,, \tag{1}$$

which is the so-called Nielsen model.

Although the above derivation is quite simple, in reality it predicates on some important assumptions. Strictly speaking, we have partitioned our planar polymer matrix into an infinite collection of thin slices, with length $\hat{l}_c$ and width proportional to the particle' length. Then, averaging has been carried out over such a thin slice which has been i) randomly selected and ii) deemed to be representative.

The assumption that the polymer matrix has an infinite extension in the normal direction is crucial on two fronts. First, it asserts that there are no boundary effects so that averaging is translation invariant and can be performed in a randomly selected thin slice without loss of generality. Second, due to the absence of boundary effects, the flow of gas molecules is local, *i.e.* it does not depend on scales other than the particles' length and width. This is a crucial observation that will become more relevant in the next section.

Equation (1) predicts that tortuosity scales linearly in both the volume fraction ϕ_p and the aspect ratio a_p. The asymptotic arguments of [17] suggest that the validity of the Nielsen model is formally limited to the so-called dilute regime, *i.e.* $a_p\phi_p << 1$.

On the other hand, the following criticism appears to have merit. Ostensibly, the Nielsen model does not hold in the three dimensional case and this raises questions on its domain of validity. However, it turns out that equation (1) is valid in three dimensions as well provided that the three dimensional particles have an infinite height $\hat{H}_p = \infty$. With this assumption, it is straightforward to show that, for a homogeneous dispersion of such particles, the averaging arguments mentioned above carry over thereby leading once more to equation (1). Numerical evidence corroborating this assertion have been presented, among others, in [7] and more recently in [8].

Two limiting cases are also of interest. The first limit concerns the case $\phi_p = 0$. In this case, the Nielsen model recovers the correct value of tortuosity, *i.e.* $\tau_N = 1$, as expected. The second limiting case is more involved. As ϕ_p approaches unity, the particles cover the whole polymer matrix and, in turn,

this implies that $l_p \to \infty$ and by extension,

$$\lim_{\phi_p \to 1} \frac{\hat{l}_p}{\hat{l}_c} = \infty \,.$$

One, therefore, expects that at this limit, tortuosity becomes unbounded and that

$$\lim_{\phi_p \to 1} \tau_N = \infty \,.$$

However, the Nielsen model predicts a finite value for tortuosity as $\phi_p \to 1$.

Interestingly, even though tortuosity converges to a wrong value, the overall gas permeability goes to zero as expected. To see this, we start from the fundamental relation that, under steady state conditions and in the absence of fillers, gas permeability ($\hat{P}$) equals solubility ($\hat{S}$) times diffusivity ($\hat{D}$) or mathematically $\hat{P} = \hat{S}\hat{D}$. Note that permeability here refers to membrane permeability, typically measured in Barrer, as opposed hydrodynamic permeability that has dimensions of Darcy units or m^2.

In the presence of additive fillers, we have $\hat{P}_{\phi_p} = \hat{S}_{\phi_p}\hat{D}_{\phi_p}$, where the subscript ϕ_p designates the dependence on volume fraction ϕ_p. Now, under the assumption that inclusion of fillers leaves the polymer matrix properties invariant [18], the solubility of the polymer-filled system scales linearly with porosity, $\hat{S}_{\phi_p} = \hat{S}(1 - \phi_p)$. Further, if we use equation (1), then $\hat{D}_{\phi_p} = \hat{D}/\tau_N$. It readily follows that,

$$\hat{P}_{\phi_p} = \hat{S}(1 - \phi_p)\frac{\hat{D}}{\tau_N} \,, \tag{2}$$

which of course goes to zero as $\phi_p \to 1$ independently of the behavior of τ_N.

This apparent rectification is actually deceiving since tortuosity continues to converge to the wrong value. Importantly, augmenting equation (1) with additional polynomial terms via appropriate Taylor or asymptotic expansions is unlikely to recover the correct limiting behavior for a finite number of terms. This is indeed the case with most tortuosity correlations that we are acquainted with, which constitute polynomial or rational extensions of the Nielsen model; see, for instance, [19, 20, 17, 21, 18].

Reconciling the good predictive capacity of the Nielsen model with the correct limiting behavior of tortuosity suggests that equation (1) is actually a systematic truncation of a more general function of the Krieger-Dougherty kind. Krieger-Dougherty functions are routinely encountered in the study of viscosity of non-colloidal suspensions [22]. Such functions are generically described by the following formula,

$$f_{KG}(\phi_p) = 1 + \hat{\lambda}_1 \frac{\phi_p^{\hat{\lambda}_2}}{(\phi_{\max} - \phi_p)^{\hat{\lambda}_3}}\,, \tag{3}$$

where $\hat{\lambda}_1, \hat{\lambda}_2, \hat{\lambda}_3 \in \mathbb{R}^+$ are coefficients and $0 < \phi_{\max} \leq 1$ stands for the maximum packing fraction. Evidently, $\hat{\lambda}_1$ should be a function of the aspect ratio a_p.

In order for the Taylor series of (3) to include a linear term, so that at least formally we can recover the Nielsen model, we should set $\hat{\lambda}_2 = 1$. We can also put bounds on $\hat{\lambda}_3$ as follows. Consider equation (2) with a more general tortuosity expression τ but such that

$$\lim_{\phi_p \to 1} \tau < \infty$$

. Clearly, the only term that drives the overall permeability to zero is the factor $(1 - \phi_p)$ and, therefore, that $\hat{P}_{\phi_p} \to 0$ at a rate $O(1 - \phi_p)$. Now, according to experimental results, reported among others, in [3, 7, 23], that cover the dilute, semi-dilute and concentrated regime (up to around $\phi_p = 0.4$), the predicted rate $O(1 - \phi_p)$ can explain reasonably well the convergence of permeability to zero. If we now consider again equation (2) but with a tortuosity expression τ_∞ such that

$$\lim_{\phi_p \to 1} \tau = +\infty$$

, then it follows that τ_{infty} has to diverge to infinity with a sub-linear rate. In other words, experiments dictate that in equation (3), $\hat{\lambda}_3 < 1$.

3. Tortuosity and the Darcy-Brinkman equations

Our next step is to derive tortuosity formulas by assuming that the polymer-filled system is actually a plane channel filled with a porous medium. With this

ansatz, the porous skeleton is determined by the geometric properties and the volume fraction of the additive fillers whereas the polymer is treated as the "empty" part of the channel where flow occurs. Then, we consider a type of fluid flow through this channel, the characteristics of which will be determined in due course, and calculate appropriately averaged velocity fields without a porous medium, $\langle \hat{u}_0 \rangle$ and with a porous medium, $\langle \hat{u}_{\phi_p} \rangle$. The ratio $\frac{\langle \hat{u}_0 \rangle}{\langle \hat{u}_{\phi_p} \rangle}$, or its dimensionless analogue, constitutes an approximation of tortuosity.

We recall that in the derivation of the Nielsen model, (1), we have considered a planar channel having length $\hat{l}_c$ in the streamwise ($\hat{x}_1$) and infinite width (or being periodic) in the normal ($\hat{x}_3$) direction. For our case, we will also consider a planar channel which has a length $\hat{l}_c$ but additionally finite width $\hat{w}_c$ with $\hat{w}_c >> \hat{l}_c$. In this matter, our channel constitutes a two dimensional cut of a typical polymeric film sample; such samples are rectangular with width and height ranging from 0.1 to 0.15cm and thickness (height) of around $50 - 100$ μm.

In this channel, we consider the fully-developed plane Poiseuille flow of a gas having density $\hat{\rho}$ and viscosity $\hat{\mu}$, induced by a forcing term $\hat{F} = -\frac{\mathrm{d}\hat{p}}{\mathrm{d}\hat{x}_1}$. The Reynolds number $Re = \frac{\hat{\rho}\hat{U}_ref\hat{w}_c/2}{\hat{\mu}}$, with $\hat{U}_ref = \frac{\hat{F}\hat{l}_c}{32\hat{\mu}}$, attains a prescribed value in the laminar regime; see below for more details. A no-slip boundary condition is applied at the walls of the channel and the overall extend of the channel in the $\hat{x}_3$ direction goes from $-\hat{w}_c/2$ to $\hat{w}_c/2$ with the origin lying in the middle of the channel. Under standard non-dimensionalization, as is well known, the velocity profile is parabolic and its non-dimensional expression reads $u(x_3) = \frac{ReF}{2}(1 - x_3^2)$.

Now, tortuosity is by definition an averaged quantity so it is natural to average the above formula for our purposes. As mentioned in the previous section, the Nielsen model employs averaging over thin slices of width proportional to the length of the particles. With this in mind we proceed as follows. Let $0 < \epsilon \leq 1$ be an arbitrary number, large enough so that a continuum description of the flow through the porous medium is still valid. With respect to the latter requirement, it is interesting to note that previous studies with granular materials, and

solids with voids more generally, have shown that the continuum limit can be surprisingly low, spanning a handful of particle diameters, [24, 25, 26]; in other words, the lower bound of ϵ can really be remarkably, albeit not arbitrarily, small.

We then average according to the following formula

$$\langle u_0^\epsilon \rangle = \frac{1}{2\epsilon} \int_{-\epsilon}^{\epsilon} \frac{ReF}{2}(x_3^2 - 1)\mathrm{d}x_3 = \frac{ReF}{2\epsilon}\frac{\epsilon^3 - 3\epsilon}{3}\,. \tag{4}$$

Next, in the same channel we regularly disperse a collection of monodisperse, rectangular fillers with length $\hat{L}_p$ and width $\hat{W}_p$, such that $\hat{L}_p, \hat{W}_p << \hat{w}_c$ and non-dimensionally $L_p, W_p << 2$. Moreover, the fillers are placed so that their length is perpendicular to the streamwise direction in accordance to Figure 1. The overall volume fraction of the fillers is $\phi_p > 0$ and, therefore, the channel is now fully covered with a porous medium that has constant porosity $\phi_f = 1 - \phi_p$.

We again consider the fully-developed plane Poiseuille flow of the same gas with the same forcing term $\hat{F}$ and the same boundary conditions. Herein, we assume that the particle Reynolds number $Re_p = \frac{\hat{\rho} U_{ref} \hat{d}_p}{\hat{\mu}}$, with $\hat{d}_p = \sqrt{\hat{L}_p^2 + \hat{W}_p^2}$ being the particle diameter, is small enough that the flow remains laminar and that it can be described by the Darcy–Brinkman equations, *i.e.* $Re_p < 50$ and Forchheimer effects are negligible [27]. The governing equations in non-dimensional form read,

$$\frac{\phi_f}{Re}\frac{\mathrm{d}^2 u}{\mathrm{d}x_3^2} - \phi_f F - \delta u = 0\,, \tag{5}$$

with δ designating the interphasial drag coefficient. Several empirical correlations have thus far been proposed for δ and the interested reader is referred to [28, 29, 30, 31, 32] for more information. Although a direct comparison between the different correlations does reveal important differences, all correlations share fundamental similarities as well as inverse dependence on the (equivalent) particle diameter and by extension the particle Reynolds number Re_p and ii) divergence to infinity as $\phi_p \to 1$. With this in mind, herein, we choose to adopt one of the simplest correlations namely the Ergun equation [33] which, in the

low Reynolds number regime and with our non-dimensionalization, reads

$$\delta = \frac{150}{Re}\frac{\phi_p^2}{\phi_f^3 \chi^2}\,. \tag{6}$$

In the above equation χ stands for the spherical equivalent particle diameter of the particles, defined as the diameter of a sphere that has the same volume to surface ratio as the particles that constitute the skeleton of the porous medium.

Now, in our case, we are working with two dimensional fillers and in order to calculate χ we need a three–dimensional extension. In order to facilitate comparison, we employ the three-dimensional extension of the Nielsen model as a guideline. In this respect, we assume that our particles are actually cuboid particles whose height equals the extension of the channel,*i.e.* $H_p = 2$. By so doing, we enforce that the gaseous molecules cannot circumvent the particles in the (fictitious) third dimension. Then, by definition, we have,

$$\begin{aligned} \frac{\frac{\pi\chi^3}{6}}{\pi\chi^2} &= \frac{2W_pL_p}{2(W_pL_p + 2W_p + 2L_p)} \Longrightarrow \\ \chi &= \frac{3L_p}{a_p + L_p/2 + 1}\,, \end{aligned} \tag{7}$$

where, as above, a_p stands for the aspect ratio. Equation (5) admits a closed form solution which reads,

$$u(x_3) = \frac{-ReF\left(1 + e^{2\sqrt{\frac{150\phi_p^2}{\phi_f^4\chi^2}}} - e^{-\sqrt{\frac{150\phi_p^2}{\phi_f^4\chi^2}}(x_3-1)} - e^{\sqrt{\frac{150\phi_p^2}{\phi_f^4\chi^2}}(1+x_3)}\right)}{\frac{150\phi_p^2}{\phi_f^4\chi^2}\left(1 + e^{2\sqrt{\frac{150\phi_p^2}{\phi_f^4\chi^2}}}\right)}\,. \tag{8}$$

Next, we recall the ϵ number used in (4) and analogously obtain the ϵ-averaged

value of (8) so that,

$$\langle u^{\epsilon}_{\phi_p}\rangle = \frac{1}{2\epsilon}\int_{-\epsilon}^{\epsilon} \frac{-ReF\left(1+e^{2\sqrt{\frac{150\phi_p^2}{\phi_f^4\chi^2}}}-e^{-\sqrt{\frac{150\phi_p^2}{\phi_f^4\chi^2}}(x_3-1)}-e^{\sqrt{\frac{150\phi_p^2}{\phi_f^4\chi^2}}(1+x_3)}\right)}{\frac{150\phi_p^2}{\phi_f^4\chi^2}\left(1+e^{2\sqrt{\frac{150\phi_p^2}{\phi_f^4\chi^2}}}\right)}\mathrm{d}x_3$$

$$= \frac{1}{2\epsilon}\left(\frac{2ReF\,\mathrm{sech}\left(\sqrt{\frac{150\phi_p^2}{\phi_f^4\chi^2}}\right)\sinh\left(\sqrt{\frac{150\phi_p^2}{\phi_f^4\chi^2}}\epsilon\right)}{\left(\frac{150\phi_p^2}{\phi_f^4\chi^2}\right)^{3/2}}-\frac{2ReF\epsilon}{\frac{150\phi_p^2}{\phi_f^4\chi^2}}\right). \tag{9}$$

We can now approximate the tortuosity as the ratio of the two average velocities so that,

$$\tau_{DB}\approx\frac{\langle u_0^{\epsilon}\rangle}{\langle u_{\phi_p}\rangle} = \frac{\frac{ReF}{2\epsilon}\frac{\epsilon^3-3\epsilon}{3}}{\frac{1}{2\epsilon}\left(\frac{2ReF\,\mathrm{sech}\left(\sqrt{\frac{150\phi_p^2}{\phi_f^4\chi^2}}\right)\sinh\left(\sqrt{\frac{150\phi_p^2}{\phi_f^4\chi^2}}\epsilon\right)}{\left(\frac{150\phi_p^2}{\phi_f^4\chi^2}\right)^{3/2}}-\frac{2ReF\epsilon}{\frac{150\phi_p^2}{\phi_f^4\chi^2}}\right)}$$

$$\frac{\left(3\epsilon-\epsilon^3\right)\left(\frac{150\phi_p^2}{\phi_f^4\chi^2}\right)^{3/2}}{6\left(\sqrt{\frac{150\phi_p^2}{\phi_f^4\chi^2}}\epsilon-\mathrm{sech}\left(\sqrt{\frac{150\phi_p^2}{\phi_f^4\chi^2}}\right)\sinh\left(\sqrt{\frac{150\phi_p^2}{\phi_f^4\chi^2}}\epsilon\right)\right)}. \tag{10}$$

The above formula is quite generic and, importantly, has an inherently correct behavior at the two limits, independently of the value of ϵ. Indeed, it is rather straightforward to show that as $\phi_p \to 0$ and $\phi_p \to 1$, $\tau_{DB} \to 1$ and $\tau_{DB} \to \infty$, respectively, which confirms our assertion. However, equation (10) is quite complicated to be directly compared to the Nielsen model or any of the alternative correlations for tortuosity and we still need to prescribe ϵ a concrete value prior performing our comparison.

We first recall that typical film samples for the measurement of permeability, which is our targeted area application, are rectangular with a dimension of around $0.1-0.15$cm whilst the additive particles have a length of approximately

10^{-5}m, [34]. If we set

$$M = \sqrt{\frac{150\phi_p^2(a_p + 1 + L_p/2)^2}{9\phi_f^4 L_p^2}}\,, \tag{11}$$

it can readily verified that for any value of a_p and for particle volume fractions $\phi_p > 10^{-4}$, $M = O(100)$. In other words, the Darcy–Brinkman equation is, in our case, singularly perturbed with respect to the parameter M; We note that M is actually the inverse of the Darcy number written in terms of porosity, and not permeability. According to the asymptotic analysis of [11] and [12], the corresponding boundary layers scale with $1/M$.

With the above in mind, the next step is to assign ϵ a specific value. The choice of ϵ is a crucial step in our analysis because, due to the macroscopic nature of the Darcy-Brinkman equation, there is an inherent effect of the channel diameter; we note that this is not case with sub-pore models, e.g. in [14]. Removing the effects of the channel diameter amounts to averaging in a way that removes the effects of the boundaries. Consequently, ϵ should a assume the following form

$$\epsilon = 1 - g(\phi_p, L_p, a_p)\frac{1}{M} = 1 - O(1/M)\,. \tag{12}$$

Here, $g(\phi_p, L_p, a_p)$ is a function to be determined. Now, since $\epsilon = 1 - O(1/M^*)$ we can Taylor expand (10) around $\epsilon = 1$ and, upon ignoring terms of order $O(\epsilon - 1)^3$ and higher, we arrive at,

$$\tau_{DB} \approx \frac{M^3}{3(M - 3\tanh(M))} + \frac{M^3((M^2+3)\tanh(M) - 3M)}{6(M - \tanh(M))^2}(\epsilon - 1)^2 \tag{13}$$

Second, in the above equation and given the magnitude of M, we can use the approximation $\tanh(M) \approx 1$ and, subsequently, Taylor expand the result at the limit $M \to \infty$ (formally at $1/M = 0$). This procedure yields, up to $O(M^2)$,

$$\tau_{DB} \approx \frac{M^3}{6}(\epsilon - 1)^2\,. \tag{14}$$

We next introduce (12) to (14) which results in,

$$\tau_{DB} \approx \frac{M^3}{6} g(\phi_p, L_p, a_p)\frac{1}{M^2}\,. \tag{15}$$

What is left, is to determine the function $g(\phi_p, L_p, a_p)$. We use as a guidance equation (3) and the subsequent discussion as follows. Let, $C_1 \in \mathbb{R}^+$ and $0 < C_2 < 1/2$. Then, if we choose $g(\phi_p, L_p, a_p)$ such that,

$$g(\phi_p, L_p, a_p) = \frac{\sqrt{6}}{M}\sqrt{\frac{150}{9}\frac{\phi_p^2(a_p + L_p/2 + 1)^2 C_1 + \phi_f^{4C_2}}{\phi_f^{4C_2}}}\,, \tag{16}$$

then simple algebra asserts that,

$$\tau_{DB} \approx 1 + C_1\sqrt{\frac{150}{9}}\frac{\phi_p(a_p + L_p/2 + 1)}{\phi_f^{2C_2}} \approx 1 + C_1\sqrt{\frac{150}{9}}\frac{\phi_p(a_p + 1)}{\phi_f^{2C_2}}\,, \tag{17}$$

where in the last approximation we have used the fact that $L_p << 1$. Equation (17) constitutes the final relation of our analysis. As requested, it depends only on the porosity of the porous medium (or the volume fraction, equivalently) and the aspect ratio of the particles that constitute the porous skeleton. Further, it inherently behaves correctly at both the lower and higher limits, $\phi_p \to 0$ and $\phi_p \to 1$, respectively. Also, its rate of convergence towards infinity is sub-linear.

On the other hand, it is clear that, unless further exogenous constraints are imposed, the averaging length is not uniquely defined. In turn, this gives rise to multiple formulas for tortuosity. We may note that this is not surprising given that tortuosity is an averaged quantity and as such is quite sensitive in the type of averaging performed.

4. Comparative study & implications

We now advert to the comparison the tortuosity formula (17) with that of the Nielsen model (1). For the sake of convenience, we juxtapose them here,

$$\tau_N = 1 + \frac{1}{2}\phi_p a_p\,, \tag{18}$$

$$\tau_{DB} = 1 + C_1\sqrt{\frac{150}{9}}\frac{\phi_p(a + 1)}{\phi_f^{2C_2}}\,. \tag{19}$$

We can now prove the following proposition

Proposition 1. *Let a_p be a fixed aspect ratio. Further, let ϕ_p^0 be an arbitrary volume fraction value. Then, for every $\varepsilon > 0$ there exist $C_1(a_p, \phi_p^0, \varepsilon)$ and $C_2(a_p, \phi_p^0, \varepsilon)$ such that*

$$|\tau_N - \tau_{DB}| << \varepsilon, \qquad \forall \phi_p < \phi_p^0 . \tag{20}$$

Proof. We first Taylor expand expand (19) around $\phi_p = 0$. Then we have, up to order $O(\phi_p^3)$,

$$\begin{aligned} &|\tau_{DB} - \tau_N| \qquad (21)\\ &= |1 + C_1\sqrt{\frac{150}{9}}(a_p+1)(\phi_p + 2C_2\phi_p^2 + O(\phi_p^3) - (1 + \frac{1}{2}\phi_p a_p)| \\ &= |(a_p C_1\sqrt{\frac{150}{9}} + C_1\sqrt{\frac{150}{9}} - \frac{a_p}{2})\phi_p + (a_p+1)C_1 2C_2\sqrt{\frac{150}{9}}\phi_p^2 + C_1 O(\phi_p^3)| \\ &= |(a_p C_1\sqrt{\frac{150}{9}} + C_1\sqrt{\frac{150}{9}} - \frac{a_p}{2})\phi_p| + |(a_p+1)C_1 4C_2\sqrt{\frac{150}{9}}\phi_p^2| + |C_1 O(\phi_p^3)| . \qquad (22) \end{aligned}$$

Now, let $\varepsilon > 0$ and fix ϕ_p^0 as an upper limit of the particle volume fractions considered, *i.e.* $\phi_p < \phi_p^0$. We want to choose C_1 and C_2 such that,

$$|(a_p C_1\sqrt{\frac{150}{9}} + C_1\sqrt{\frac{150}{9}} - \frac{a_p}{2})\phi_p| < \frac{\varepsilon}{3} \tag{23}$$

$$|(a_p+1)C_1 2C_2\sqrt{\frac{150}{9}}\phi_p^2| < \frac{\varepsilon}{3} \tag{24}$$

$$|C_1 O(\phi_p^3)| < \frac{\varepsilon}{3} . \tag{25}$$

Solving the first inequality in terms of C_1 readily yields that

$$C_1 < \left(\frac{\varepsilon}{3\phi_p^0} + \frac{a_p}{2}\right)\sqrt{\frac{9}{150}}\frac{1}{a_p+1} . \tag{26}$$

Accordingly, the second inequality asserts that, for C_2,

$$C_2 < \frac{\varepsilon}{6\phi_p^0(a_p+1)C_1}\sqrt{\frac{9}{150}} . \tag{27}$$

With this choice of C_1 and C_2 it is straighforward to show that

$$|C_1 O(\phi_p^3)| < \frac{\varepsilon}{3} \tag{28}$$

is also true. The proof is completed upon combining inequalities (26)-(28). □

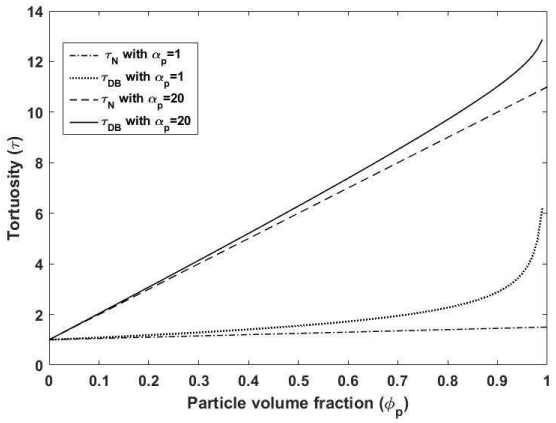


Figure 2: Tortuosity predictions of the of the Nielsen model (τ_N) and ones of equation (19) (τ_{DB}) for $\varepsilon = 0.1$ and $\phi_p^0 = 0.1$ and C_1, C_2 chosen according to Proposition 1. The two cases correspond to $\alpha_p = 1$ and $\alpha_p = 20$.

The above proposition asserts that the Nielsen model is indeed a truncated version of the tortuosity formulas derived from the Darcy–Brinkman equation. This is also visually demonstrated in Figure 2 where the tortuosity predictions of the Nielsen model (τ_N) are superimposed the ones of equation (19) (τ_{DB}) for two representative cases, namely $\alpha_p = 1$ and $\alpha_p = 20$. Moreover, we have set $\varepsilon = 0.1$ and $\phi_p^0 = 0.1$ and C_1, C_2 are chosen so as to verify the inequalities of Proposition 1. We can readily confirm that, as asserted by Proposition 1, τ_N remains ε–close to τ_{DB} up until ϕ_p^0 and higher particle volume fractions they two expressions progressively diverge from each other.

A direct juxtaposition of the tortuosity formula (19) to the Ergun equation (6) that has been employed as a model of the interphasial drag asserts the following: the tortuosity formulas that we have dealt with in this study are actually lower-order approximations of the interphasial drag coefficient, averaged out over appropriate ranges. In fact, for constant porosity, a closer inspection of the Darcy-Brinkman equation readily reveals that it is only the interphasial drag coefficient that can induce velocity profiles different from the ones obtained via the Navier–Stokes equations. Besides the obvious practical applications of

this observation, *i.e.* one needs "only" an accurate expression of the interphasial drag coefficient and then is able to compute tortuosity, a natural physical justification also exists. In continuum models for flows in porous media, momentum exchanges the between the solid phase (porous medium) and the fluid phase (pure fluid) comprise two terms a) the interphasial drag and b) a gyroscopic, nozzling term [35, 36]. In the homogenized view of such continuum theories the interphasial drag decelerates the velocity, and upon zooming in we can convince ourselves that this deceleration is the macroscopic manifestation of longer fluid trajectories due to the presence of the porous skeleton; the relation of the latter has been unraveled in the works of [13, 14, 16, 15], therefore, the presence study bridges the gap at the macroscopic level.

The last comment concerns the robustness and limitations of the present study. The first point of concern is the choice of different correlations for the interphasial drag coefficient. As we mentioned above, a quick inspection of the available correlations asserts the following: i) all correlations that extend to very low porosities (or high volume fractions) follow a Krieger-Dougherty-type functional relation and blow-up as $\phi_p \to 1$. ii) all correlations exhibit a inverse quadratic relation to the particle diameter (microscopic length scale) as this stems invariant geometric arguments. In fact, and especially in the laminar regime, most correlations differ only in their multiplicative constants, typically obtained through fitting against available experimental measurements. In other words, the analysis employed herein is ostensibly not affected by the particular choice of the correlation for the interphasial drag coefficient, modulo the constants.

Another limitation stems from the domain of validity of the governing equations. We have opted to work with the Darcy–Brinkman equation so that the foregoing are formally valid for particle Reynolds number up to (around) $Re_p \sim 50$. When the particle Reynolds number becomes larger the interphasial drag needs to accommodate for quadratic velocity effects and the appropriate governing equations are the so-called Darcy–Brinkman–Forchheimer equations [37, 38]. These equations, however, are not always solvable in closed form and,

therefore, one needs to numerically integrate them and perform a numerical replication of our analysis.

A third limitation concerns the value of the parameter M and its "avatar" M^*. In our case, $M >> 1$ which has allowed us to perform an asymptotic analysis of the solution profiles. However, there are cases where the channel diameter is not much larger than the particle one. In such cases, one can longer Taylor expand (10) around the value $\epsilon = 1$ and, therefore, the subsequent analysis is no longer valid. In fact, such cases stand at the borderline of the validity regime of continuum approximation and, as such, are more amenable to numerical simulations via Lattice-Boltzman methods.

A last limitation concerns the ostensibly two-dimensional nature of our results. Equation (19) formula was derived based on three-dimensional cuboids, having a practically infinite extension in the transverse direction. The general three-dimensional case will generate additional length scales, for instance in the calculation of the spherically equivalent diameter, that will complicate the analysis though in principle the main steps should remain invariant.

Before concluding the manuscript a comment on the applicability of equation (19) is also in order. Our tortuosity formula is based on a number of simplified assumptions that, clearly, act as limiting factors concerning its practical applicability. Nevertheless, within its domain of validity, and assuming that C_1 and C_2 have been retrofitted with some preliminary experiments, equation (19) can be utilized for the estimation of tortuosity in applications that involve polymer-filled systems, e.g. rigid and flexible packaging. More specifically, it can provide useful estimates of worst-case (or best–case) scenarios with little effort.

5. Conclusion

In the present study, we have shown that the well-known Nielsen model for the calculation of tortuosity in polymer–filled systems can be rediscovered if the polymer-filled system is treated as a porous medium and the flow is modeled via the Darcy-Brinkman equation. It is shown that, if velocity profiles are averaged

over a subtly defined range, inspired by boundary layer theory, a general formula for tortuosity is obtained that is valid at both the limits of particle volume fraction approaching zero and unity.

We have additionally elaborated on the limitations of our analysis that directly determine the range of processing conditions that our tortuosity formula can be employed. Within its domain of validity, the derived tortuosity formula can be utilized provided that accurate expressions for the interphasial drag coefficient are available.

Coupling tortuosity with hydrodynamics is not new in the literature. As we mentioned in the introduction of this manuscript, previous studies have already calculated tortuosity by using sub-porous scale simulations via Lattice-Boltzman methods. The present study constitutes the macroscopic analogue of these earlier efforts and, therefore, provides additional physical insights stemming from the continuum approach. Most importantly, it is shown that, due to the homogenized nature of our equations, the tortuosity expression is closely related to the interphasial drag.

Acknowledgements

The authors would like to thank the anonymous Reviewers whose comments and suggestions have helped improving the quality of the manuscript.

[1] D. Paul, L. Robeson, Polymer nanotechnology: Nanocomposites, Polymer 49 (2008) 3187–3204.

[2] S. Ray, M. Okamoto, Polymer/layered silicate nanocomposites: a review from preparation to processing, Progress in Polymer Science 28 (2003) 1539–1641.

[3] G. Choudalakis, A. Gotsis, Permeability of polymer/clay nanocomposites: A review, European Polymer Journal 45 (4) (2009) 967 – 984.

[4] J. P. R.M. Barrer, Diffusion in heterogeneous media: lattice and parallelepipeds in a continuous phase, British Journal of Applied Physics 12 (1961) 691–697.

[5] C. Wolf, H. Angellier-Coussy, N. Gontard, F. Doghieri, V. Guillard, How the shape of fillers affects the barrier properties of polymer/non-porous particles nanocomposites: A review, Journal of Membrane Science 556 (2018) 393 – 418.

[6] L. Nielsen, Models for the permeability of filled polymer systems, Journal of Macromolecular Science A 1 (1967) 929–942.

[7] A. Gusev, H. Lusti, Rational design of nanocomposites for barrier applications, Advanced Materials 13 (21) (2001) 1641–1643.

[8] M. Minelli, M. G. Baschetti, F. Doghieri, A comprehensive model for mass transport properties in nanocomposites, Journal of Membrane Science 381 (1) (2011) 10 – 20.

[9] Y. Cui, S. Kumar, B. Rao Kona, D. van Houcke, Gas barrier properties of polymer/clay nanocomposites, RSC Advances 5 (2015) 63669–63690.

[10] B. Tan, N. Thomas, A review of the water barrier properties of polymer/clay and polymer/graphene nanocomposites, Journal of Membrane Science 514 (2016) 595 – 612.

[11] K. Hooman, A perturbation solution for forced convection in a porous-saturated duct, Journal of Computational and Applied Mathematics 211 (1) (2008) 57 – 66.

[12] J. P. Kelliher, R. Temam, X. Wang, Boundary layer associated with the Darcy–Brinkman–Boussinesq model for convection in porous media, Physica D: Nonlinear Phenomena 240 (7) (2011) 619 – 628.

[13] T. Rosén, J. Eller, J. Kang, N. I. Prasianakis, J. Mantzaras, F. N. Büchi, Saturation dependent effective transport properties of pefc gas diffusion layers, Journal of The Electrochemical Society 159 (9) (2012) F536–F544.

[14] N. I. Prasianakis, T. Rosén, J. Kang, J. Eller, J. Mantzaras, F. N. Büichi, Simulation of 3d porous media flows with application to polymer electrolyte fuel cells, Communications in Computational Physics 13 (3) (2013) 851866.

[15] Y. Yang, R. A. Patel, S. V. Churakov, N. I. Prasianakis, G. Kosakowski, M. Wang, Multiscale modeling of ion diffusion in cement paste: electrical double layer effects, Cement and Concrete Composites 96 (2019) 55 – 65.

[16] S. V. Churakov, N. I. Prasianakis, Review of the current status and challenges for a holistic process-based description of mass transport and mineral reactivity in porous media, American Journal of Science 318 (9) (2018) 921–948.

[17] G. Fredrickson, J. Bicerano, Barrier properties of oriented disk composites, Journal of Chemical Physics 110 (1999) 2181–2188.

[18] E. Picard, A. Vermogen, J.-F. Grard, E. Espuche, Barrier properties of nylon 6-montmorillonite nanocomposite membranes prepared by melt blending: Influence of the clay content and dispersion state: Consequences on modelling, Journal of Membrane Science 292 (1) (2007) 133 – 144.

[19] W. Brydges, S. Gulati, G. Baum, Permeability of glass ribbon-reinforced composites, Journal of Membrane Science 10 (1975) 2044–2049.

[20] E. Cussler, S. Hughes, W. Ward, R. Aris, Barrier membranes, Journal of Membrane Science 38 (1988) 161–174.

[21] N. Lap, E. Nuxoll, E. Cussler, Polydisperse flakes in barrier films, Journal of Membrane Science 236 (2004) 29–37.

[22] M. M. Denn, J. F. Morris, Rheology of non-brownian suspensions, Annual Review of Chemical and Biomolecular Engineering 5 (1) (2014) 203–228.

[23] E. Dunkerley, D. Schmidt, Effects of composition, orientation and temperature on the o2 permeability of model polymer/clay nanocomposites, Macromolecules 43 (24) (2010) 10536–10544.

[24] M. A. Goodman, S. C. Cowin, A continuum theory for granular materials, Archive for Rational Mechanics and Analysis 44 (4) (1972) 249–266.

[25] S. L. Passman, J. W. Nunziato, E. K. Walsh, A Theory of Multiphase Mixtures, Springer New York, New York, NY, 1984, pp. 286–325.

[26] D. Monsorno, C. Varsakelis, M. Papalexandris, Poiseuille flow of dense non-colloidal suspensions: The role of intergranular and nonlocal stresses in particle migration, Journal of Non-Newtonian Fluid Mechanics 247 (2017) 229 – 238.

[27] D. Lasseux, F. J. Valdés-Parada, On the developments of darcy's law to include inertial and slip effects, Comptes Rendus Mécanique 345 (9) (2017) 660 – 669, a century of fluid mechanics: 18701970.

[28] S. Benyahia, M. Syamlal, T. J. O'Brien, Extension of hillkochladd drag correlation over all ranges of reynolds number and solids volume fraction, Powder Technology 162 (2) (2006) 166 – 174.

[29] J. Lundberg, B. M Halvorsen, A review of some existing drag models describing the interaction between phases in a bubbling fluidized bed, Proc. Proc. 49th Scand. Conf. Simulation and Modeling.

[30] P. D. Antoniadis, M. V. Papalexandris, Dynamics of shear layers at the interface of a highly porous medium and a pure fluid, Physics of Fluids 27 (1) (2015) 014104.

[31] C. M. R. Luna, L. R. Carrocci, G. L. Arce, I. vila, A comparative assessment of empirical and lattice boltzmann method-based drag models for simulation of gassolid flow hydrodynamics in a bubbling fluidized bed, Particuology 33 (2017) 129 – 137.

[32] R. Stanly, G. Shoev, Detailed analysis of recent drag models using multiple cases of mono-disperse fluidized beds with geldart-b and geldart-d particles, Chemical Engineering Science 188 (2018) 132–149.

[33] S. Ergun, Fluid flow through packed columns, Chemical Engineering Progress 48 (1952) 89–94.

[34] B. Morris, The Science and Technology of Flexible Packaging: Multilayer Films from Resin and process to End Use, Elsevier, Oxford, U.K., 2017.

[35] M. Papalexandris, P. Antoniadis, A thermo-mechanical model for flows in superposed porous and fluid layers with interphasial heat and mass exchange, International Journal of Heat and Mass Transfer 88 (2015) 42 – 54.

[36] P. D. Antoniadis, M. V. Papalexandris, Numerical study of unsteady, thermally-stratified shear flows in superposed porous and pure-fluid domains, International Journal of Heat and Mass Transfer 96 (2016) 643 – 659.

[37] N. Kladias, V. Prasad, Experimental verification of Darcy-Brinkman-Forchheimer flow model for natural convection in porous media, Journal of Thermophysics and Heat Transfer 5 (4) (1991) 560–576.

[38] C. Varsakelis, M. V. Papalexandris, On the well-posedness of the Darcy–Brinkman–Forchheimer equations for coupled porous media-clear fluid flow, Nonlinearity 30 (4) (2017) 1449–1464.